Photoinduced valence dynamics in $EuNi_2(Si_{0.21}Ge_{0.79})_2$ studied via time-resolved x-ray absorption spectroscopy

Y. Yokoyama,[1,2,*] K. Kawakami,[3] Y. Hirata,[1,2] K. Takubo,[1,†] K. Yamamoto,[1,2,‡] K. Abe,[3] A. Mitsuda,[4] H. Wada,[4] T. Uozumi,[3] S. Yamamoto,[1,2] I. Matsuda,[1,2] S. Kimura,[5,6] K. Mimura,[3] and H. Wadati[1,2,§]

[1]*Institute for Solid State Physics, University of Tokyo, Chiba 277-8581, Japan*
[2]*Department of Physics, University of Tokyo, Tokyo 113-0033, Japan*
[3]*Graduate School of Engineering, Osaka Prefecture University, Sakai 599-8531, Japan*
[4]*Department of Physics, Kyushu University, Fukuoka 819-0395, Japan*
[5]*Graduate School of Frontier Biosciences, Osaka University, Suita 565-0871, Japan*
[6]*Department of Physics, Graduate School of Science, Osaka Unviersity, Toyonaka 560-0043, Japan*

(Received 10 May 2019; revised manuscript received 30 July 2019; published 12 September 2019)

The photoinduced valence dynamics of $EuNi_2(Si_{0.21}Ge_{0.79})_2$ were investigated using time-resolved x-ray absorption spectroscopy for Eu M_5 edge. Through the pump-probe technique with synchrotron x-ray and Ti:sapphire laser pulses, a photoinduced valence transition was observed from Eu^{3+} to Eu^{2+}. Because the lifetime of a photoinduced state can be up to 3 ns, a metastable state is considered to be realized. By comparing the experimental results with the theoretical calculations, the photoinduced valence transition between Eu $4f$ and conduction electrons was quantitatively evaluated.

DOI: 10.1103/PhysRevB.100.115123

I. INTRODUCTION

The unique phenomena exhibited by $4f$ electron systems, such as valence fluctuation, valence transition, and the Kondo effect, have drawn the attention. These phenomena originate from the hybridization between $4f$ electrons and conduction electrons [1]. Recently, the valence fluctuation and transition in Ce- and Yb-based compounds have reportedly exhibited unconventional superconductivity and non-Fermi-liquid behavior [2–7]. In addition, the valence fluctuation has been related to quantum critical phenomena [8]. Therefore the mechanisms of valence fluctuation and transition are germane to the understanding of $4f$ electron systems.

For the study of the valence fluctuation and the valence transition, Eu compounds are one of the most suitable specimens due to their significantly large valence change. The valence fluctuation and valence transition have been observed between Eu^{2+} ($4f^7$, $J = 7/2$) and Eu^{3+} ($4f^6$, $J = 0$) ions [9–21]. The transition of the Eu mean valence occurs by external stimuli such as temperature [9,11,12,14–21], magnetic field [13,15,20], and/or pressure [14,16]. The detection of valence transitions was achieved using the Eu M_5-edge x-ray absorption spectroscopy (XAS) [18,19]. However, the interaction of the Eu compounds with photon irradiation is not fully understood. Photon-controlled hybridization between the $4f$ and conduction electrons may help realize a novel state and unravel more information on electron-photon interaction. Therefore, in this study, the photoinduced dynamics of electronic structures were investigated.

Extensive studies on photoinduced transition in strongly correlated $3d$ transition metal compounds were performed using pump-probe x-ray spectroscopies, revealing dynamics such as insulator-to-metal transition [22–26]. These techniques involve controlling the time difference between a pump light, such as an visible laser pulse, and a probe light, such as a synchrotron radiation x-ray pulse, to detect the time-dependent variation of photoinduced electronic structures. In the soft x-ray region, the $3d$ states were directly observed through the $2p \rightarrow 3d$ resonance [25]. As for the $4f$ rare-earth compounds, the spin states and the hybridization between $4f$ electrons and conduction electrons were studied via resonant x-ray diffraction with $3d \rightarrow 4f$ resonance [27] and reflectivity measurements [28]. Although the valence of $4f$ electron systems were clearly distinguished in XAS spectra, the valence dynamics were not observed via XAS measurements. Therefore the photoinduced valence dynamics were investigated using time-resolved soft x-ray absorption spectroscopy (Tr-XAS).

II. EXPERIMENTAL

For the study of photoinduced valence dynamics, $EuNi_2(Si_{1-x}Ge_x)_2$ with $x = 0.79$ was selected as it exhibits a large valence change (∼0.6), and the valence transition occurs at a relatively high temperature (∼84 K) [21]. As the surface of $EuNi_2(Si_{0.21}Ge_{0.79})_2$ is sensitive to oxygen, i.e.,

*Present address: Japan Synchrotron Radiation Research Institute (JASRI), Sayo 679-5198, Japan; y.yokoyama@spring8.or.jp
†Present address: Department of Chemistry, Tokyo Institute of Technology, Meguro, Tokyo 152-8551, Japan.
‡Present address: Department of Materials Molecular Science, Institute for Molecular Science, Myodaiji-cho, Okazaki, Aichi 444-8585, Japan.
§Present address: Graduate School of Material Science, University of Hyogo, 3-2-1, Koto, Kamigori-cho, Ako-gun, Hyogo 678-1297, Japan.

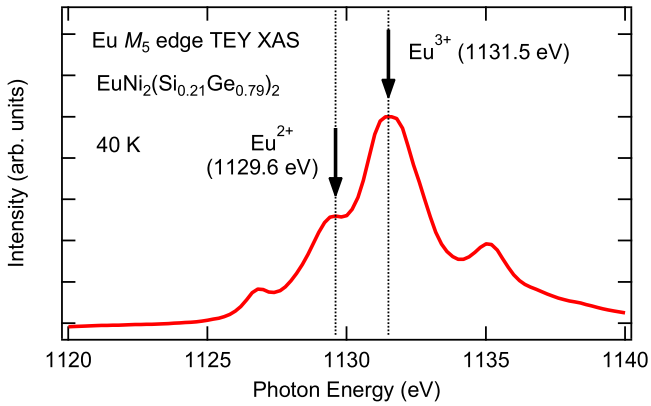

FIG. 1. Eu M_5-edge TEY XAS spectra of $EuNi_2(Si_{0.21}Ge_{0.79})_2$ at 40 K. Arrows indicate the characteristic peaks of Eu^{2+} at 1129.6 eV and Eu^{3+} at 1131.5 eV.

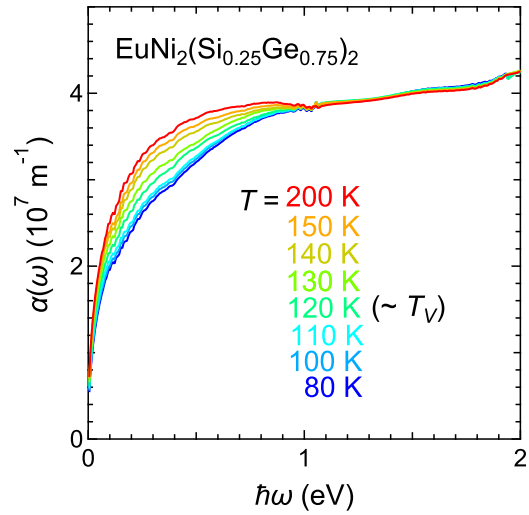

FIG. 2. Absorption coefficient spectra of $EuNi_2(Si_{0.25}Ge_{0.75})_2$ at several temperatures from the Kramers-Kronig analysis of reflectivity spectra reported in Ref. [31]. T_v denotes the valence transition temperature.

it tends to get oxidized, the polycrystalline samples were fractured prior to the measurements in an ultra-high vacuum chamber at the possible lowest temperature (∼40 K). The static XAS and Tr-XAS measurements were performed at BL07LSU of SPring-8 [26,29,30]. For the static XAS of Eu M_5 edge, the measurements were performed at 40 K by the total electron yield (TEY) mode with an ammeter. Because the response time of an ammeter is larger than the order of ps, the partial electron yield (PEY) mode was instead used with a microchannel plate (MCP) detector for Tr-XAS [26].

III. RESULTS AND DISCUSSION

In the first step, the static XAS measurement of $EuNi_2(Si_{0.21}Ge_{0.79})_2$ was performed using the TEY mode. Figure 1 shows the Eu M_5-edge TEY XAS spectrum at 40 K. The shape of the spectrum was in good agreement with that in Ref. [19], indicating the fine quality of the fractured sample surface. From the atomic multiplet calculations in Ref. [18], the peaks at 1129.6 and 1131.5 eV originate from the Eu^{2+} and Eu^{3+} components, respectively.

Based on the result of static XAS, Tr-XAS measurements were performed using the pump-probe technique. The schematic diagram of the experimental setup is shown in Fig. 3(a). A Ti:sapphire laser pulse ($h\nu = 1.5$ eV, repetition rate = 1 kHz, width = 50 fs) was adopted as the pump light for this study. As a probe light, a synchrotron soft x-ray pulse (an isolated bunch in the H mode of SPring-8: A single bunch + a bunch train) with energy near Eu M_5 edge was used. The incident angle of the x ray was parallel to the sample surface normal, while that of the laser was set as 10° below the x ray. In the related Eu compounds, the reflectivity of 1.5 eV laser is ∼60% [31,32]. The spot size of the x rays and the laser was ∼100 μm × 5 μm and ∼600 μm × 600 μm, respectively. In soft x-ray region, the absorption length is > 100 nm and the probing depth of electron yield is ∼4 nm [33,34]. On the other hand, the absorption length of the laser was obtained from the absorption coefficient in a related Eu compound. Figure 2 shows the absorption coefficient spectra in $EuNi_2(Si_{0.25}Ge_{0.75})_2$ at several temperatures below and above the valence transition temperature (T_v), which is derived from the Kramers-Kronig analysis of reflectivity spectra reported in Ref. [31]. Since the coefficient is $\sim 4 \times 10^7$ m^{-1} at 1.5 eV, the absorption length of Ti:sapphire laser is ∼25 nm. As the area probed with PEY was fully exposed by the laser irradiation, the dynamics induced by the pure laser incidence were probed. By varying the delay time between the x-ray and the laser pulses, time-resolved information could be obtained [30]. In our experiment, the zero point of the delay time was evaluated by fitting of a delay time scan after being roughly determined with a photodiode and an oscilloscope. A time resolution of 50 ps was decided by considering the width of the synchrotron x-ray pulse [29,30].

For evaluating the time-resolved change of the XAS intensity, an oscilloscope was used. The signals of MCP were input into the oscilloscope through an ac coupled circuit and an amplifier. The output on the oscilloscope during the time-resolved measurements is shown in Fig. 3(b). The solid and dotted lines correspond to the conditions of "X-ray: ON, laser: ON" and "X-ray: OFF, laser: ON", respectively. The solid line indicates the bunches in H-mode detected mainly as photoelectrons from the sample. On the other hand, the dotted line suggests the background originated from laser irradiation (such as stray light) and/or electronic noises. The variations of voltage at ∼ − 3000 and ∼100 ns were considered to be noises associated with the laser irradiation. To remove these background noises, the dotted line was subtracted from the solid line. After the removal of the background, for evaluating the area of the bunches, we set the baseline of the pumped bunch and the reference bunch as zero, respectively. The intensity of the XAS was obtained from the area of the pumped bunch (after laser irradiation) and the reference bunch (before laser irradiation). Then, the rate of change was calculated by dividing the area of the pumped bunch by that of the reference bunch. It should be noted that the sample quality (broken or not) can be verified by evaluating the reference bunch.

Figure 4(a) shows the Tr-XAS intensity probed at the energy for Eu^{2+} (1129.6 eV) and Eu^{3+} (1131.5 eV). The

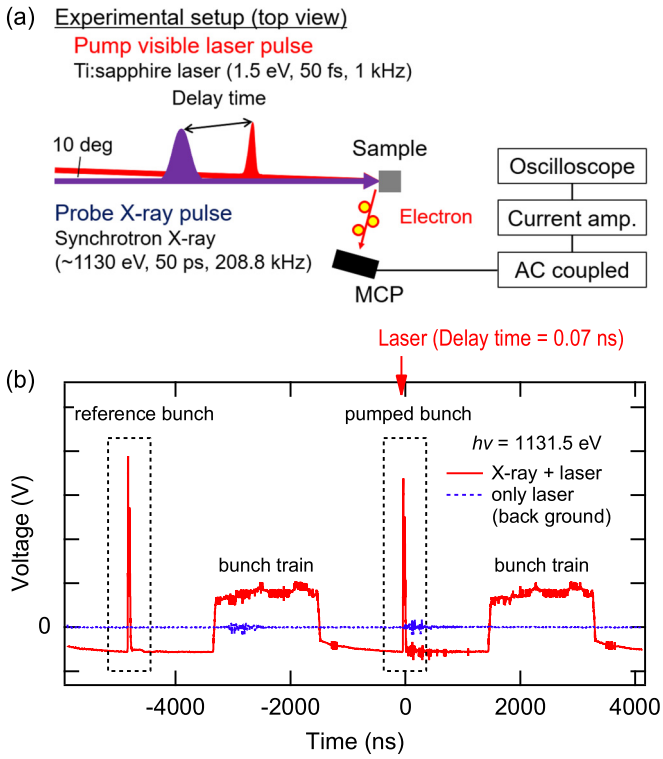

FIG. 3. (a) Schematic diagram of setup for the pump-probe technique. The incident visible laser and x-ray pulses were overlapped at the sample surface. The delay time was defined as the time difference between the visible pump laser pulse and the probe x-ray pulse. (b) MCP output on the oscilloscope during the time-resolved measurements at a delay time = 0.07 ns. The incident x-ray energy was set to 1131.5 eV (Eu^{3+}). Solid and dotted lines correspond to "X-ray: ON, laser: ON" and "X-ray: OFF, laser: ON", respectively. The arrow indicates the laser position. The results were integrated over several thousand iterations.

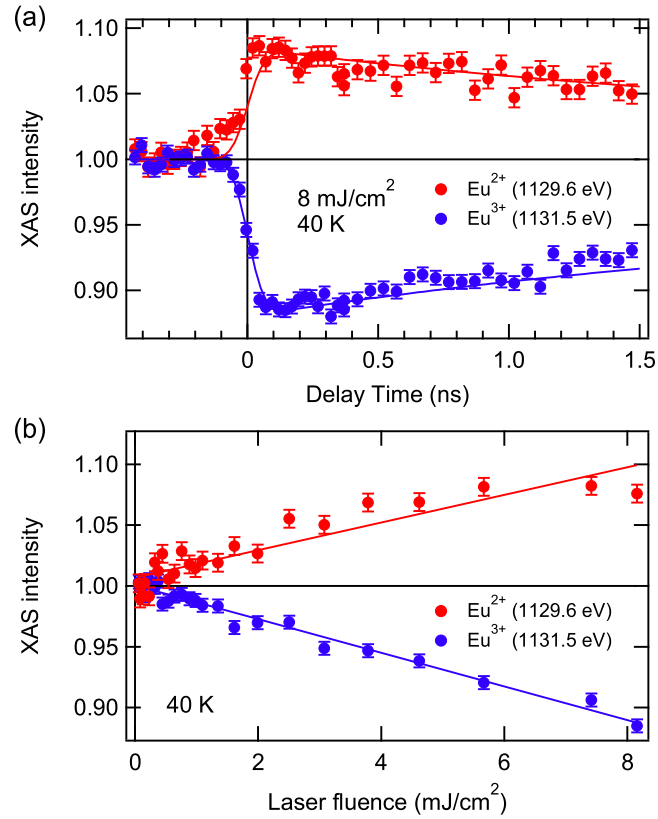

FIG. 4. (a) Tr-XAS intensity for Eu^{2+} (1129.6 eV) and Eu^{3+} (1131.5 eV) obtained by the PEY mode. Dots and lines represent the experimental and fitting results. The measurements were performed at 40 K under the 1.5 eV laser irradiation with a fluence of ~8 mJ/cm^2. Delay time was defined as the time difference between the synchrotron x-ray and laser pulse. The zero point of the delay time was determined from the fitting results. The error bars were obtained from the standard deviation of the intensity at negative delay times smaller than −0.15 ns. (b) Laser fluence dependence of XAS intensity in $EuNi_2(Si_{0.21}Ge_{0.79})_2$ probed for Eu^{2+} (1129.6 eV) and Eu^{3+} (1131.5 eV) obtained by the PEY mode. During the measurements, the delay time was fixed at 0.07 ns. Dots represent the experimental results and lines denote the fitting results.

sharp increase in intensity of XAS for Eu^{2+} was observed by ~10% after a delay =0 ns, which suggests an increase in the ratio of Eu^{2+} by the laser irradiation. On the other hand, the intensity of Eu^{3+} decreased by ~10% just after the laser irradiation. These results suggest the mean valence of Eu becomes closer to Eu^{2+} by laser irradiation, indicating a photoinduced valence transition between Eu $4f$ and its conduction electrons. The timescale of photoinduced valence dynamics was also evaluated using the following function:

$$I(t) = \begin{cases} 1 & (t \leqslant 0) \\ I_1 \exp(-t/\tau_{\text{change}}) + I_2[1 - \exp(-t/\tau_{\text{recovery}})]. \\ +1 - I_1 & (t > 0) \end{cases} \quad (1)$$

There was a slower (>10 ns) recovery component which might correspond to thermal transport and the recovery was not completed in several dozens of nanoseconds. Then, for obtaining the timescale of the valence transition with separating the slower component, we evaluated the intensity of change and recovery as I_1 and I_2, respectively. Because the time resolution of Tr-XAS was ~50 ps, the function was convoluted with the Gaussian response function (τ_{Gauss} = 50 ps). From the fitting results represented by solid lines in Fig. 4(a), τ_{change} was found to be faster than 50 ps and τ_{recovery} was ~3 ns. As the timescale of valence transition was much longer than a few ps, reported for $YbAgCu_4$ and $YbInCu_4$ via photoinduced reflectivity measurements [28], a photoinduced metastable state might be realized in $EuNi_2(Si_{0.21}Ge_{0.79})_2$.

The laser fluence dependence was also investigated. For those measurements, the delay time was fixed at 0.07 ns because the biggest changes were observed at that delay time. Figure 4(b) shows the laser fluence dependence of XAS intensity probed at the peak energies of Eu^{2+} (1129.6 eV) and Eu^{3+} (1131.5 eV). The fluence dependence can be fitted by a straight line, and there is no threshold, such as the photoinduced insulator-to-metal transition [25], which indicates that the valence of Eu can change by weaker laser fluence. However, the valence change by temperature should have a

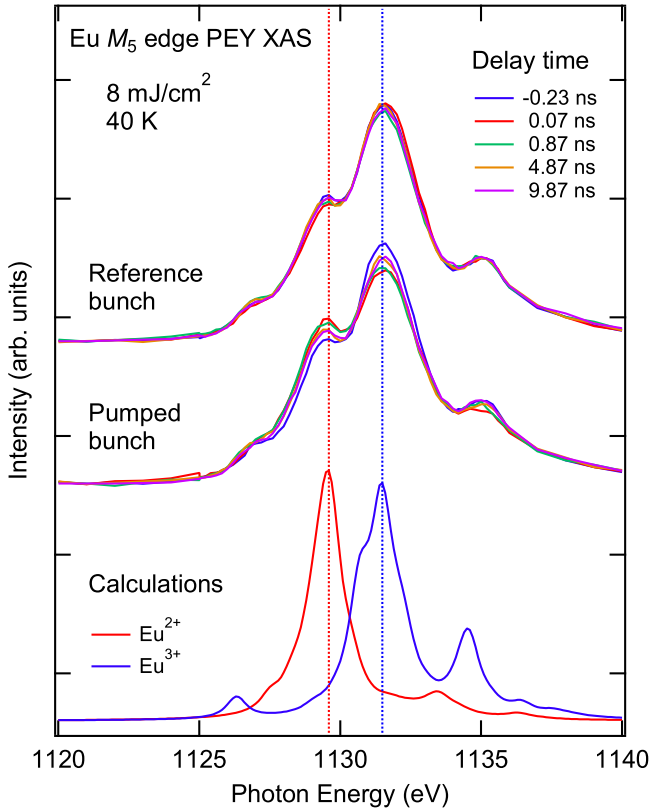

FIG. 5. Eu M_5-edge PEY XAS spectra of $EuNi_2(Si_{0.21}Ge_{0.79})_2$ at various delay times. The peaks at 1129.6 and 1131.5 eV correspond to the main peaks of Eu^{2+} and Eu^{3+}, respectively. The theoretical spectra were obtained by intra-atomic multiplet calculations of Eu^{2+} and Eu^{3+} from Ref. [18].

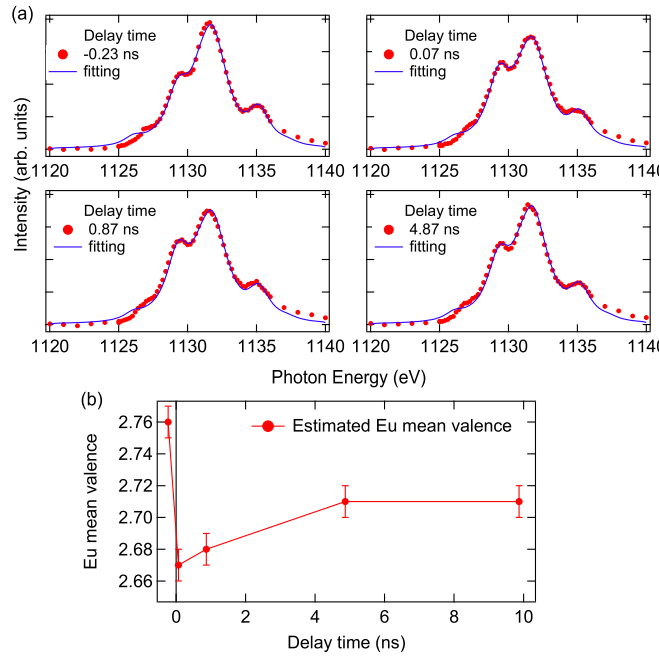

FIG. 6. (a) Comparison between the experimental Eu M_5-edge PEY XAS spectra of $EuNi_2(Si_{0.21}Ge_{0.79})_2$ at various delay times (dotted lines), and the theoretical spectra reproduced by the linear combinations of Eu^{2+} and Eu^{3+} (solid lines). (b) The time-dependent variation of the mean valence of Eu evaluated by the calculations. The error bars were obtained from the variation of the reference bunch spectra in Fig. 5.

threshold because the valence of Eu changes drastically near the transition temperature, as shown in Ref. [21]. Therefore, a unique photoinduced valence transition is considered.

To investigate the photoinduced valence dynamics in further detail, the PEY XAS spectra were measured at different delay times. Figure 5 shows the Eu M_5-edge PEY XAS spectra at delay times $= -0.23$, 0.07, 0.87, 4.87, and 9.87 ns. The peaks at 1129.6 and 1131.5 eV correspond to the main peaks of Eu^{2+} and Eu^{3+}, respectively. As for the reference bunches, the spectra were almost the same, indicating that the samples did not deteriorate during the measurements. By changing the delay times between the laser and x-ray pulses, the shapes of XAS spectra can be changed, which corresponds to the photoinduced valence dynamics between Eu^{2+} and Eu^{3+}. Later, the mean valence of Eu was evaluated using the theoretical spectra obtained by the intra-atomic multiplet calculations of Eu^{2+} and Eu^{3+} from Ref. [18].

Figure 6(a) shows the comparison of the experimental Eu M_5-edge PEY XAS spectra at various delay times with the theoretical spectra. The valence of Eu was evaluated by comparing it with the linear combinations of the theoretical spectra for Eu^{2+} and Eu^{3+}. As shown in the figure, the theoretically reproduced spectra were in good agreement with the experimental ones. The evaluated valence of Eu at various delay times are shown in Fig. 6(b). Before the laser irradiation, the valence of Eu was 2.76 ± 0.01. The value is almost the same as 2.78 ± 0.02 at 50 K in Ref. [21]. Upon the irradiation of the laser pulse, the valence changes to 2.67 ± 0.01 at the delay time $= 0.07$ ns, indicating photoinduced valence transition. Then, the valence gradually recovered to its initial value, as shown in the figure.

The observed Tr-XAS intensity in Fig. 4(a) is interpreted as the variation of Eu valence via XAS spectrum at each interval of the delay time. Since the each intensity is convoluted with 50 ps, it includes the information at faster and slower delay times. By comparing the XAS spectra at several delay times with the theoretical spectra, the photoinduced valence transition from 2.76 to 2.67 was revealed. Referring to the temperature increase of a metallic material with a visible laser [35], the temperature of the electron is considered to increase to several hundreds K. Since the change and the recovery of the electron temperature can be completed within a few picoseconds [35,36], the XAS intensity convoluted with 50 ps may become smaller than the original one. However, the lifetime as long as $\sim$3 ns is much longer than the time resolution of our experiments and then implies the existence of a photoinduced metastable state. Although the temperature is considered to increase to several hundreds K by the laser irradiation with 8 mJ/cm^2, the XAS intensity is proportional to the laser fluence and the behavior is clearly different from the valence change by temperature. Then, the behavior of the fluence dependence also suggests a different phenomenon from the temperature-induced valence transition, which is realized by the temperature change ($\Delta T \sim 10$ meV) because of a hybridization change coupled to a Kondo-like volume

collapse [18,21]. Considering that the energy difference between Eu^{2+} and Eu^{3+} is the order of 1 eV [18], the valence transition with the 1.5 eV laser can be a different process from the temperature-induced one. In addition, from the band calculation of $EuNi_2Ge_2$ in Ref. [37], there are several Eu $4f$ states between ± 1.5 eV. Therefore a metastable state, i.e., a mixed state of Eu^{2+} splitted by the crystal field and Eu^{3+}, is considered to be realized with the 1.5 eV laser irradiation. Since the Ti:sapphire laser pulse energy of 1.5 eV is close to the plasma frequency in the optical conductivity [31], this energy may also be important to realize the metastable state. Faster timescale measurements using x-ray free electron laser or femtoslicing technique can help further investigation of the photoinduced state.

IV. CONCLUSIONS

To summarize, static XAS and Tr-XAS measurements of $EuNi_2(Si_{0.21}Ge_{0.79})_2$ were performed at BL07LSU of SPring-8. From the static XAS, the characteristic peaks of Eu^{2+} at 1129.6 eV and Eu^{3+} at 1131.5 eV were observed. In the Tr-XAS measurements, the photoinduced valence dynamics between Eu^{2+} and Eu^{3+} were detected successfully. The timescales of valence dynamics were evaluated, and those for change and recovery were found to be shorter than 50 ps and longer than 3 ns. The laser fluence dependence was also measured. In the absorption spectra observed at different delay times, the mean valence of Eu was evaluated using the theoretical spectra, revealing a valence change of $\sim$0.1. These characteristics are different from the valence transition by external stimuli such as temperature, indicating the novel photoinduced states.

ACKNOWLEDGMENTS

This work was supported by MEXT Quantum Leap Flagship Program (MEXT Q-LEAP) Grant No. JPMXS0118068681 and by JSPS KAKENHI Grant No. 19H05824, and carried out by the joint research in the Synchrotron Radiation Research Organization and the Institute for Solid State Physics, the University of Tokyo (Proposals No. 2017A7403, No. 2017B7403, and No. 2018B7578).

[1] C. M. Varma, Rev. Mod. Phys. **48**, 219 (1976).
[2] D. Jaccard, H. Wilhelm, K. Alami-Yadri, and E. Vargoz, Physica B **259-261**, 1 (1999).
[3] O. Trovarelli, C. Geibel, S. Mederle, C. Langhammer, F. M. Grosche, P. Gegenwart, M. Lang, G. Sparn, and F. Steglich, Phys. Rev. Lett. **85**, 626 (2000).
[4] A. T. Holmes, D. Jaccard, and K. Miyake, Phys. Rev. B **69**, 024508 (2004).
[5] A. T. Holmes, D. Jaccard, and K. Miyake, J. Phys. Soc. Jpn. **76**, 051002 (2007).
[6] S. Nakatsuji, K. Kuga, Y. Machida, T. Tayama, T. Sakakibara, Y. Karaki, H. Ishimoto, S. Yonezawa, Y. Maeno, E. Pearson, G. G. Lonzarich, L. Balicas, H. Lee, and Z. Fisk, Nat. Phys. **4**, 603 (2008).
[7] S. Watanabe and K. Miyake, J. Phys.: Condens. Matter **23**, 094217 (2011).
[8] K. Kuga, Y. Matsumoto, M. Okawa, S. Suzuki, T. Tomita, K. Sone, Y. Shimura, T. Sakakibara, D. Nishio-Hamane, Y. Karaki, Y. Takata, M. Matsunami, R. Eguchi, M. Taguchi, A. Chainani, S. Shin, K. Tamasaku, Y. Nishino, M. Yabashi, T. Ishikawa, and S. Nakatsuji, Sci. Adv. **4**, eaao3547 (2018).
[9] E. V. Sampathkumaran, L. C. Gupta, R. Vijayaraghavan, K. V. Gopalakrishnan, R. G. Pillay, and H. G. Devare, J. Phys. C **14**, L237 (1981).
[10] M. Croft, J. A. Hodges, E. Kemly, A. Krishnan, V. Murgai, and L. C. Gupta, Phys. Rev. Lett. **48**, 826 (1982).
[11] C. U. Segre, M. Croft, J. A. Hodges, V. Murgai, L. C. Gupta, and R. D. Parks, Phys. Rev. Lett. **49**, 1947 (1982).
[12] G. Wortmann, I. Nowik, B. Perscheid, G. Kaindl, and I. Felner, Phys. Rev. B **43**, 5261 (1991).
[13] A. Mitsuda, H. Wada, M. Shiga, H. A. Katori, and T. Goto, Phys. Rev. B **55**, 12474 (1997).
[14] H.-J. Hesse, R. Lubbers, M. Winzenick, H. Neuling, and G. Wortmann, J. Alloys Compd. **246**, 220 (1997).
[15] H. Wada, A. Nakamura, A. Mitsuda, M. Shiga, T. Tanaka, H. Mitamura, and T. Goto, J. Phys.: Condens. Matter **9**, 7913 (1997).
[16] H. Wada, M. F. Hundley, R. Movshovich, and J. D. Thompson, Phys. Rev. B **59**, 1141 (1999).
[17] H. Wada, T. Sakata, A. Nakamura, A. Mitsuda, M. Shiga, Y. Ikeda, and Y. Bando, J. Phys. Soc. Jpn. **68**, 950 (1999).
[18] K. Yamamoto, K. Horiba, M. Taguchi, M. Matsunami, N. Kamakura, A. Chainani, Y. Takata, K. Mimura, M. Shiga, H. Wada, Y. Senba, H. Ohashi, and S. Shin, Phys. Rev. B **72**, 161101(R) (2005).
[19] K. Yamamoto, K. Horiba, M. Taguchi, M. Matsunami, N. Kamakura, Y. Takata, A. Chainani, K. Mimura, M. Shiga, H. Wada, Y. Senba, H. Ohashi, and S. Shin, Physica B **378-380**, 681 (2006).
[20] Y. H. Matsuda, T. Inami, K. Ohwada, Y. Murata, H. Nojiri, Y. Murakami, A. Mitsuda, H. Wada, H. Miyazaki, and I. Harada, J. Phys. Soc. Jpn. **77**, 054713 (2008).
[21] K. Ichiki, K. Mimura, H. Anzai, T. Uozumi, H. Sato, Y. Utsumi, S. Ueda, A. Mitsuda, H. Wada, Y. Taguchi, K. Shimada, H. Namatame, and M. Taniguchi, Phys. Rev. B **96**, 045106 (2017).
[22] I. Radu, K. Vahaplar, C. Stamm, T. Kachel, N. Pontius, H. A. Durr, T. A. Ostler, J. Barker, R. F. L. Evans, R. W. Chantrell, A. Tsukamoto, A. Itoh, A. Kirilyuk, T. Rasing, and A. V. Kimel, Nature (London) **472**, 205 (2011).
[23] P. Beaud, A. Caviezel, S. O. Mariager, L. Rettig, G. Ingold, C. Dornes, S.-W. Huang, J. A. Johnson, M. Radovic, T. Huber, T. Kubacka, A. Ferrer, H. T. Lemke, M. Chollet, D. Zhu, J. M. Glownia, M. Sikorski, A. Robert, H. Wadati, M. Nakamura, M. Kawasaki, Y. Tokura, S. L. Johnson, and U. Staub, Nat. Mater. **13**, 923 (2014).
[24] E. Jal, V. López-Flores, N. Pontius, T. Ferté, N. Bergeard, C. Boeglin, B. Vodungbo, J. Luning, and N. Jaouen, Phys. Rev. B **95**, 184422 (2017).

[25] T. Tsuyama, S. Chakraverty, S. Macke, N. Pontius, C. Schüßler-Langeheine, H. Y. Hwang, Y. Tokura, and H. Wadati, Phys. Rev. Lett. **116**, 256402 (2016).

[26] K. Takubo, K. Yamamoto, Y. Hirata, Y. Yokoyama, Y. Kubota, Sh. Yamamoto, S. Yamamoto, I. Matsuda, S. Shin, T. Seki, K. Takanashi, and H. Wadati, Appl. Phys. Lett. **110**, 162401 (2017).

[27] N. Thielemann-Kühn, D. Schick, N. Pontius, C. Trabant, R. Mitzner, K. Holldack, H. Zabel, A. Föhlisch, and C. Schüßler-Langeheine, Phys. Rev. Lett. **119**, 197202 (2017).

[28] M. Y. Zhang, R. Y. Chen, T. Dong, and N. L. Wang, Phys. Rev. B **95**, 165104 (2017).

[29] S. Yamamoto, Y. Senba, T. Tanaka, H. Ohashi, T. Hirono, H. Kimura, M. Fujisawa, J. Miyawaki, A. Harasawa, T. Seike, S. Takahashi, N. Nariyama, T. Matsushita, M. Takeuchi, T. Ohata, Y. Furukawa, K. Takeshita, S. Goto, Y. Harada, S. Shin, H. Kitamura, A. Kakizaki, M. Oshima, and I. Matsuda, J. Synchrotron Radiat. **21**, 352 (2014).

[30] M. Ogawa, S. Yamamoto, Y. Kousa, F. Nakamura, R. Yukawa, A. Fukushima, A. Harasawa, H. Kondo, Y. Tanaka, A. Kakizaki, and I. Matsuda, Rev. Sci. Instrum. **83**, 023109 (2012).

[31] S. Kimura, M. Okuno, H. Iwata, T. Saitoh, T. Okuda, A. Harasawa, T. Kinoshita, A. Mitsuda, H. Wada, and M. Shiga, J. Phys. Soc. Jpn. **71**, 255 (2002).

[32] V. Guritanu, S. Seiro, J. Sichelschmidt, N. Caroca-Canales, T. Iizuka, S. Kimura, C. Geibel, and F. Steglich, Phys. Rev. Lett. **109**, 247207 (2012).

[33] F. De Groot and A. Kotani, *Core Level Spectroscopy of Solids*, (CRC Press, 2008).

[34] H. Wadati, A. J. Achkar, D. G. Hawthorn, T. Z. Regier, M. P. Singh, K. D. Truong, P. Fournier, G. Chen, T. Mizokawa, and G. A. Sawatzky, Appl. Phys. Lett. **100**, 193906 (2012).

[35] E. Beaurepaire, J.-C. Merle, A. Daunois, and J.-Y. Bigot, Phys. Rev. Lett. **76**, 4250 (1996).

[36] A. Kirilyuk, A. V. Kimel, and T. Rasing, Rev. Mod. Phys. **82**, 2731 (2010).

[37] U. B. Paramanik, A. Bar, D. Das, N. Caroca-Canales, R. Prasad, C. Geibel, and Z. Hossain, J. Phys.: Condens. Matter **28**, 166001 (2016).